ChemPubSoc Europe

DOI: 10.1002/celc.201402325

Enhancing the Electrochemical and Electronic Performance of CVD-Grown Graphene by Minimizing Trace Metal Impurities**

Rodrigo M. Iost,[a, b] Frank N. Crespilho,[b] Laura Zuccaro,[a] Hak Ki Yu,[c] Alec M. Wodtke,[c] Klaus Kern,[a, d] and Kannan Balasubramanian*[a]

The presence of unwanted impurities in graphene is known to have a significant impact on its physical and chemical properties. Similar to carbon nanotubes, any trace metals present in graphene will affect the electrocatalytic properties of the material. Here, we show by direct electroanalysis that traces of copper still remain in transferred CVD (chemical vapor deposition)-grown graphene (even after the usual copper etching process) and strongly influence its electrochemical properties. Subsequently, we use a real-time electrochemical etching procedure to remove more than 90% of the trace metal impurities, with a clear improvement in both the electrochemical and electronic-transport properties of monolayer graphene.

Graphene—with its unique physical and chemical properties—is emerging as a promising material for the next generation of electronic and electrochemical devices.[1] Since the routine possibility to isolate single flakes was reported, there has been an enormous interest in its use as an active component for applications such as field-effect transistors,[2] sensors,[3] transparent flexible electrodes for photovoltaic devices,[4] and nanoscale electrodes in electrochemistry.[5] One of the fundamental concerns when deploying graphene for electronic applications is to ensure that the active area of graphene devices is free of any kind of impurities. The presence of organic residues or local charge traps in the underlying substrate is known to significantly affect the performance of the realized devices.[6] Annealing in ultrahigh vacuum or in Ar/H_2 atmosphere removes organic impurities,[7] while the effect of the substrate can be overcome by suspended graphene[8] or graphene on hexagonal boron nitride.[9] Current-induced annealing in vacuum is an alternative, which vaporizes the impurities by local heating (up to 400–600 °C).[10] These approaches allow for a reduction in charge-carrier inhomogeneity, thereby significantly increasing the charge-carrier mobility.[11] On the other hand, when utilizing graphene for electrocatalytic or other electrochemical applications in general, it is necessary to ensure that the active element is also free of metallic impurities.[12]

Recently, it was demonstrated that traces of metal impurities in graphene obtained from the mechanical exfoliation of graphite[13] are responsible for the favorable electrocatalytic properties of graphene-based electrodes. The basis for this argument comes from the fact that some sources of graphite present trace metal contaminants,[14] which are carried over to the active regions of the final electrode, especially when realizing them in bulk form. Electrodes from individual monolayer flakes have been often realized using (chemical vapor deposition) CVD-grown graphene, which is typically grown on copper or nickel films.[15] For fabricating electrodes or devices, the underlying metal film is etched away after presenting a polymer support from the top of graphene.[16] Despite the use of rigorous etching procedures, trace metal impurities have been reported also in CVD-graphene (grown on nickel),[17] underlining a fundamental problem. By using electrochemical cycling of chemically derived graphene oxide in HNO_3, the electrocatalytic effect was found to be lower, which was attributed to removal of iron impurities.[13d] Removal of metallic traces on monolayer graphene and the effect of such metal impurities on the electronic transport in graphene has however not been reported yet.

Here we follow an in situ electrochemical etching (e-etching) procedure in acid that allows us to directly monitor the removal of trace copper impurities present on transferred graphene that was grown on copper. By means of electroanalysis, combined with surface, spectroscopic and mass spectrometric characterization, we clearly show that the parasitic electrocatalytic effects are completely removed by this e-etching procedure. The electronic transport properties also show a clear improvement in charge-carrier mobility and suppression of charge-carrier inhomogeneity upon e-etching.

First we confirm, by means of direct electroanalysis, that trace copper impurities are still present after transferring CVD-graphene[18] on to Si/SiO_2 substrates. (see the Supporting Information, SI for experimental details). The etching of copper is done in a solution of HCl with added H_2O_2. This solution en-

[a] R. M. Iost, Dr. L. Zuccaro, Prof. K. Kern, Dr. K. Balasubramanian
Max Planck Institute for Solid State Research
Heisenbergstr. 1, D70569 Stuttgart (Germany)
E-mail: b.kannan@fkf.mpg.de

[b] R. M. Iost, Prof. F. N. Crespilho
Instituto de Química de São Carlos
Universidade de São Paulo
13560-970 (Brazil)

[c] Dr. H. K. Yu, Prof. A. M. Wodtke
Max Planck Institute for Biophysical Chemistry
37077 Göttingen (Germany)

[d] Prof. K. Kern
Institut de Physique de la Matière Condensée
Ecole Polytechnique Federale de Lausanne
CH-1015, Lausanne (Switzerland)
CVD: Chemical Vapor Deposition

[**] CVD: Chemical Vapor Deposition

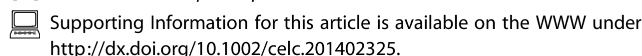
Supporting Information for this article is available on the WWW under http://dx.doi.org/10.1002/celc.201402325.

 © 2014 Wiley-VCH Verlag GmbH & Co. KGaA, Weinheim

sures a clean and efficient etching of the copper film in less than 10 min and avoids any additional metal contamination that may be introduced when using the more common etchant ferric chloride.[17] Furthermore, we do a rapid thermal annealing of the fabricated devices at 585 °C for 40 s in an argon atmosphere, to remove organic residues (comparable to the current annealing procedure). Figure 1 a shows the cyclic voltammogram (CV) of CVD-graphene after transfer (black curve I) at pH 7. Two oxidation peaks are clearly visible. They are also present in the CV of bulk copper film (along with graphene) shown for comparison (red curve II). Possible copper remains that may be present on top of graphene are etched further with an additional dip in the HCl/H_2O_2 etching solution. The CV of this graphene is shown in the blue curve III, exhibiting again the same oxidation peaks and a voltammetric profile similar to that of a bulk copper foil, albeit with a much lower current intensity.

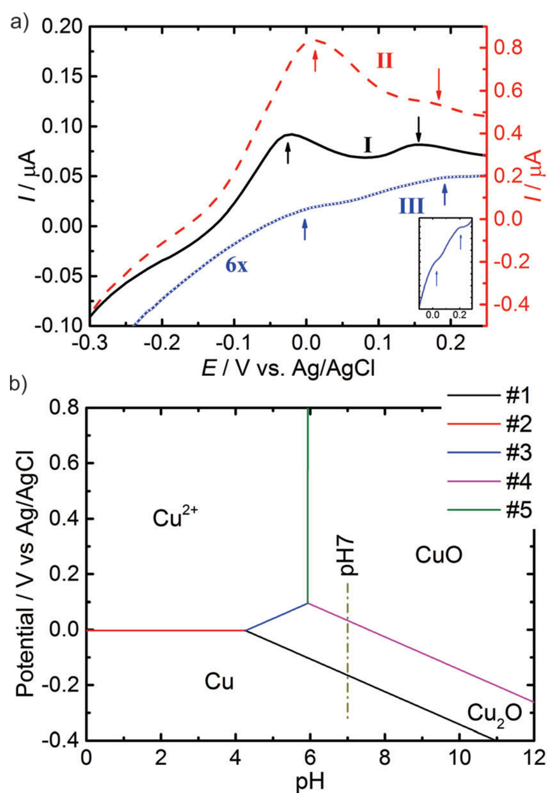

Figure 1. Electrochemistry of CVD-grown graphene: a) Cyclic voltammograms (CVs) of I) transferred CVD-graphene after etching the underlying copper foil in HCl/H_2O_2; II) graphene with copper foil as procured, and III) graphene as transferred in (I) after an additional etching in HCl/H_2O_2. The inset shows a zoomed-in region of curve (III). The arrows indicate the approximate position of the oxidation peaks (Cu^0/Cu^+ and Cu^+/Cu^{2+}). Supporting electrolyte: phosphate buffer 0.1 mol L^{-1}, pH 7, scan rate: 50 mV s^{-1}, T = 25 °C under ambient conditions (see Figure S1 for complete CVs). b) Simplified Pourbaix diagram for the Cu:H_2O system showing the redox behavior of copper as a function of applied electrochemical potential and pH. See the SI for the individual reaction steps #1 to #5.

Based on the above observations we attribute the occurrence of the oxidation peaks in curves I and III to the presence of trace copper impurities on transferred graphene. We gather support for this aspect from the Pourbaix diagram (Figure 1 b) showing the pH–potential equilibrium of solid copper in contact with water (a more detailed discussion can be found in the SI).[19] The two peaks occurring in the CVs of Figure 1 a can be directly assigned to the oxidation reactions Cu^0/Cu^+ and Cu^+/Cu^{2+}. The oxidation peaks show a slight shift in their absolute position from one sample to the other, most likely because of a slight variation in the cluster sizes and the amount and local chemical environment of the copper/copper oxide traces.[20] Moreover, we observe that the oxidation peaks shift to more negative values as we increase the pH, consistent with the Pourbaix diagram (see Figure S2). From the integrated peak intensity of the oxidation peaks (curve III) on several samples, we estimate a density of $(2.7 \pm 0.5) \times 10^{12}$ Cu atoms cm^{-2}.

Now we present the salient aspects of the e-etching procedure aimed at the removal of copper/copper oxide traces from graphene. The electrochemical corrosion of copper is well studied in acidic media with chloride ions.[21] At moderate concentrations of HCl, the anodic dissolution of copper takes place through the formation of copper chloride, which is subsequently converted to soluble Cu^{2+} ions.[21a,22] To achieve such a dissolution of the traces of copper/copper oxide on graphene, we scan the potential in the range of +/−1 V (vs. Ag/AgCl) in a solution of 10 mM or 100 mM HCl. Figure 2 a shows the CV during the first, the tenth and the 16th scans. During the first scan, an oxidation peak is visible, which is attributed to the formation of copper chloride, consistent with previous corrosion data on copper and with the Pourbaix diagram of the $Cu:Cl^-:H_2O$ system.[19,21b,22a] To favor the formation of aqueous Cu^{2+}, we scan the potential up to +1 V (vs. Ag/AgCl). By doing so, the oxidation peak of copper diminishes in intensity and finally vanishes completely in the 16th cycle. In all of the samples we have investigated, we need at most 20 cycles to remove this peak completely. The choice of HCl instead of other acids, such as H_2SO_4 or HNO_3,[13d] is because of the higher stability of graphene in HCl. In other acid media, we have observed some kind of damage to graphene, such as rolling up or the formation of cracks or holes. Moreover, cycling the potential in these acids may lead to the oxidation of graphene.[23] The removal of copper/copper oxide is further evident from the CV traces in the broader potential range shown in Figure 2 b. The current onset is at −0.25 V (vs. Ag/AgCl) before e-etching, which we attribute to water reduction.[24] The shift of the potential to more negative values (−0.39 V vs. Ag/AgCl) is consistent with a reduction of the electrocatalytic activity, confirming the removal of copper/copper oxide traces from the graphene surfaces. Further support is acquired by evaluating the electrochemical behavior of metal-free flexible carbon fibers (see SI).

We have also performed a surface and spectroscopic characterization of the graphene electrodes before and after the e-etching procedure. The atomic force microscopy (AFM) images (see Figure S5) show that there are no additional ripples or holes formed using our e-etching procedure in any of the investigated samples. Typical Raman spectra (see Figure S5) obtained after e-etching show that we have almost no intensity

© 2014 Wiley-VCH Verlag GmbH & Co. KGaA, Weinheim

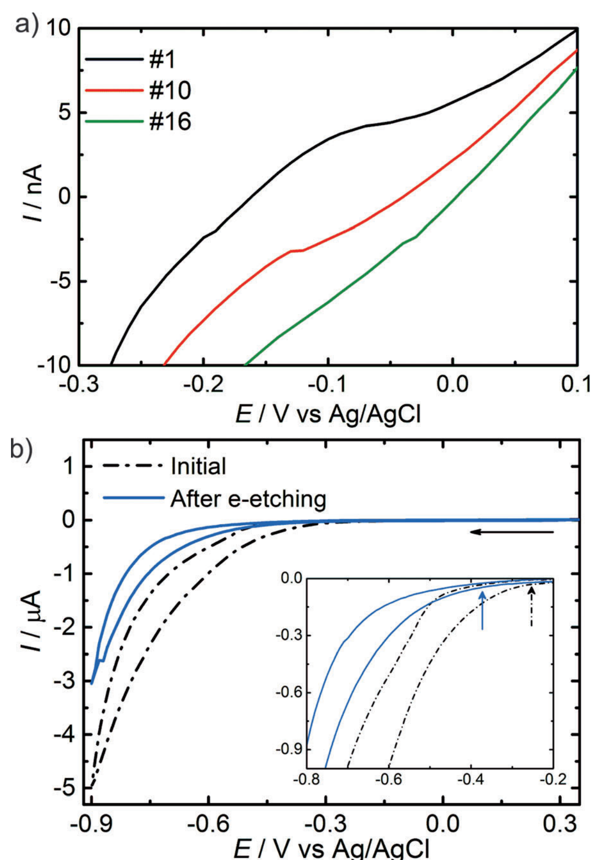

Figure 2. Electrochemical etching (e-etching) of graphene: a) CVs of transferred graphene during e-etching, whereby the potential is scanned in a range of +/−1 V (vs. Ag/AgCl) in 0.1 mol L^{-1} HCl. (see complete CVs in Figure S3). b) CV of graphene before and after e-etching in 0.1 mol L^{-1} HCl. The inset shows a zoomed-in area around the onset potential for water reduction marked by the vertical arrows; scan rate: 50 mV s^{-1}; T = 25 °C, under ambient conditions.

at the D-peak (estimated defect density: 54 to 72 nm) suggesting that the e-etching procedure does not introduce any kind of disorder or additional covalent functionalities or oxidized moieties.[25] Moreover, systematic time-of-flight secondary ion mass spectrometry (TOF-SIMS) measurements clearly show that we can remove at least 90% (at best 97%) of the copper traces on transferred graphene (see table ST1 in the SI). Based on these observations we conclude that the e-etching procedure frees graphene from metal/metal oxide impurities without affecting its physical and chemical properties.

Now, we present the effect of e-etching on the transport properties of graphene. For this purpose, we have fabricated Hall bar structures (see inset in Figure 3) on transferred graphene (see SI for experimental details).[18,26] Figure 3 presents typical results obtained before and after e-etching. The removal of copper impurities sharpens the slope of the gate dependence of the four-probe resistance (Figure 3 a) and charge-carrier density (Figure 3 b) signifying an improved gating efficiency after e-etching. The shift in the Dirac point is consistent with the removal of electron acceptors such as copper (lower work function than graphene).[27] We see an increase in the electron concentration by around 3×10^{12} cm^{-2}, consistent with the estimated density of copper atoms in Figure 1. Most importantly, Figure 3 c shows that the charge-carrier mobility values in both the hole and electron regimes are clearly enhanced (~60%) after the e-etching procedure. Moreover, we even observe a reduction of charge-carrier density around the Dirac point signifying a reduced charge inhomogeneity (~30%) there (see Figure S6).[8] Although these factors represent modest improvements, they are consistent with the reduction of additional phonon scattering (on top of scattering from SiO_2) that is most

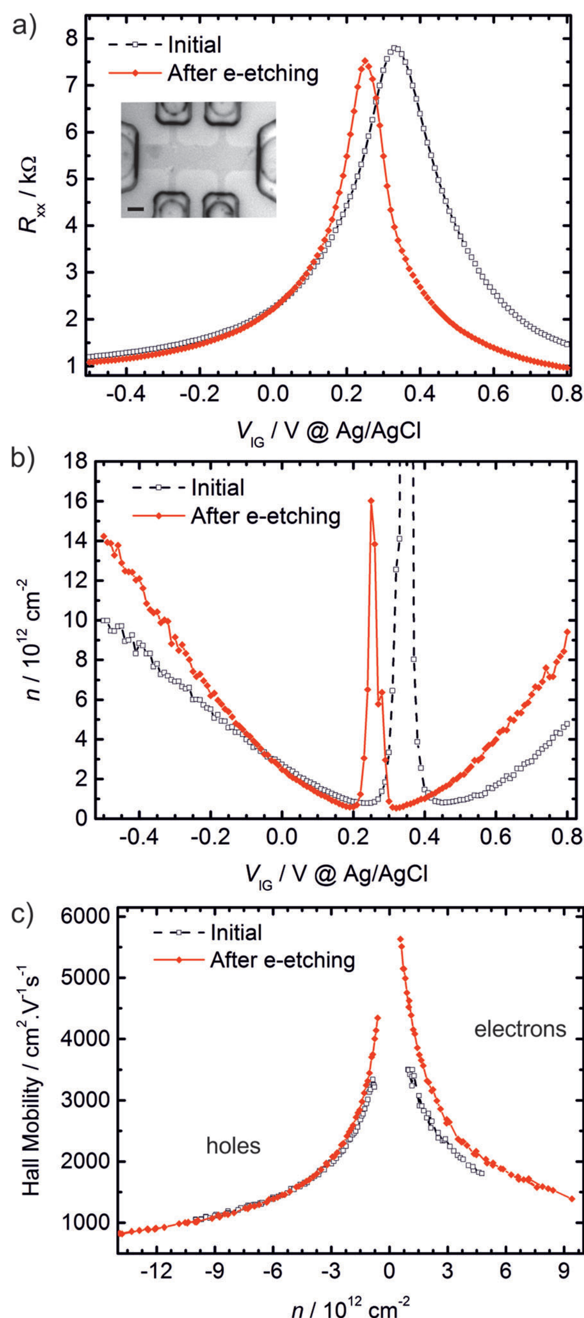

Figure 3. Electronic transport in e-etched graphene: Gate dependence of the four-probe resistance (R_{xx}) (a) and charge-carrier density (n) (b) as a function of the liquid gate voltage (at a Ag/AgCl reference). c) Hall mobility as a function of the charge-carrier concentration; in phosphate buffer solution (pH 7, 0.1 mol L^{-1}) (see also Figure S6). The inset shows the graphene Hall bar (scale bar 5 µm).

© 2014 Wiley-VCH Verlag GmbH & Co. KGaA, Weinheim

likely introduced through the trace metal impurities. Hence, the e-etching procedure, when applied to suspended CVD-graphene, may bring an additional improvement of the charge-transport properties, thereby raising hope to attain a performance approaching that of exfoliated graphene devices.

Finally, we would like to show that graphene after e-etching shows its pristine electrochemical behavior free of any parasitic electrocatalytic effects. Here, we have chosen to use two specific probes, namely, L-glutathione and cumene hydroperoxide.[12,13c,d,28] Figure 4 shows the CV of graphene in the presence

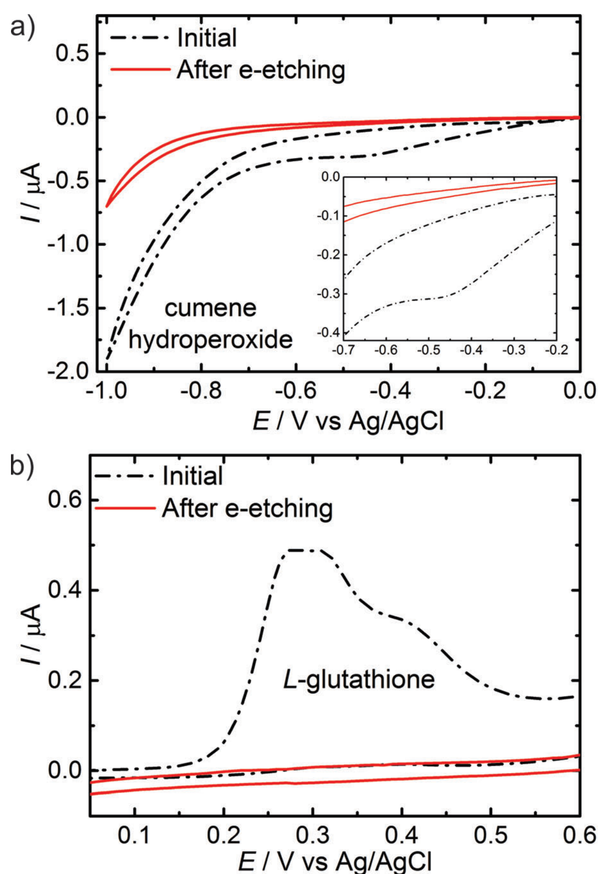

Figure 4. Electrocatalytic activity of e-etched graphene. CVs of graphene before and after e-etching in the presence of 5 mmol L^{-1} (a) cumene hydroperoxide and (b) L-glutathione. The inset in (a) shows a zoomed-in region. Supporting electrolyte: phosphate buffer 0.1 mol L^{-1}, pH 7; scan rate: 50 mV s^{-1}; $T=25\,^{\circ}C$, under ambient conditions.

of these two probes before and after e-etching. The CV before e-etching in Figure 4a shows a cathodic peak at around −0.45 V (vs. Ag/AgCl) corresponding to the reduction of cumene hydroperoxide, consistent with previous reports on graphite-based electrodes.[13c,28] Most strikingly, the peak completely disappears after the e-etching process, in addition to a shift of the onset potential for water reduction to more negative potentials. Both these aspects are consistent with the liberation of metal/metal oxide impurities from graphene, which were indeed the reason for the high initial electrocatalytic activity. Figure 4b shows a similar observation for the other probe L-glutathione. We are now left with truly pristine graphene, which does not show any parasitic electrochemical activity in a broad potential range of +/−0.75 V, as would be expected from theory for a truly basal plane of sp^2 carbon.[29]

In conclusion, we have directly detected metal traces that remain after the CVD-graphene transfer process, strongly affecting its electrochemical behavior. Removal of these traces is achieved by an electrochemical etching route with the possibility of real-time monitoring and without affecting the morphology of graphene and avoiding any additional chemical functionality. The electronic and electrochemical properties show a clear improvement, especially the complete removal of parasitic electrocatalytic behavior. The simplicity of our e-etching procedure allows for its use in a broad range of electrical and electrochemical applications to optimize device performance.

Acknowledgements

We acknowledge financial support from the Brazilian funding agency FAPESP (project numbers: 2013/14262-7, 2013/04663-4 and 2013/15443-9), U. Starke and T. Acartuerk for TOF-SIMS measurements, S. Schmid and Y. Link for metal evaporation and R. Urcuyo for discussions.

Keywords: doping · electrocatalytic activity · mobility · purification · scattering

[1] A. K. Geim, K. S. Novoselov, *Nat. Mater.* **2007**, *6*, 183–191.
[2] K. S. Novoselov, A. K. Geim, S. V. Morozov, D. Jiang, Y. Zhang, S. V. Dubonos, I. V. Grigorieva, A. A. Firsov, *Science* **2004**, *306*, 666–669.
[3] a) F. Schedin, A. K. Geim, S. V. Morozov, E. W. Hill, P. Blake, M. I. Katsnelson, K. S. Novoselov, *Nat. Mater.* **2007**, *6*, 652–655; b) K. Balasubramanian, K. Kern, *Adv. Mater.* **2014**, *26*, 1154–1175.
[4] a) C. N. R. Rao, A. K. Sood, K. S. Subrahmanyam, A. Govindaraj, *Angew. Chem. Int. Ed.* **2009**, *48*, 7752–7777; *Angew. Chem.* **2009**, *121*, 7890–7916; b) M. He, J. H. Jung, F. Qiu, Z. Q. Lin, *J. Mater. Chem.* **2012**, *22*, 24254–24264.
[5] a) B. Zhang, L. X. Fan, H. W. Zhong, Y. W. Liu, S. L. Chen, *J. Am. Chem. Soc.* **2013**, *135*, 10073–10080; b) W. Li, C. Tan, M. A. Lowe, H. D. Abruna, D. C. Ralph, *ACS Nano* **2011**, *5*, 2264–2270; c) A. T. Valota, I. A. Kinloch, K. S. Novoselov, C. Casiraghi, A. Eckmann, E. W. Hill, R. A. W. Dryfe, *ACSs Nano* **2011**, *5*, 8809–8815.
[6] a) J. H. Chen, C. Jang, S. D. Xiao, M. Ishigami, M. S. Fuhrer, *Nat. Nanotechnol.* **2008**, *3*, 206–209; b) J. H. Chen, C. Jang, M. Ishigami, S. Xiao, W. G. Cullen, E. D. Williams, M. S. Fuhrer, *Solid State Commun.* **2009**, *149*, 1080–1086.
[7] a) M. Ishigami, J. H. Chen, W. G. Cullen, M. S. Fuhrer, E. D. Williams, *Nano Lett.* **2007**, *7*, 1643–1648; b) E. Stolyarova, K. T. Rim, S. M. Ryu, J. Maultzsch, P. Kim, L. E. Brus, T. F. Heinz, M. S. Hybertsen, G. W. Flynn, *Proc. Natl. Acad. Sci. USA* **2007**, *104*, 9209–9212; c) Y. C. Lin, C. C. Lu, C. H. Yeh, C. H. Jin, K. Suenaga, P. W. Chiu, *Nano Lett.* **2012**, *12*, 414–419.
[8] K. I. Bolotin, K. J. Sikes, Z. Jiang, M. Klima, G. Fudenberg, J. Hone, P. Kim, H. L. Stormer, *Solid State Commun.* **2008**, *146*, 351–355.
[9] C. R. Dean, A. F. Young, I. Meric, C. Lee, L. Wang, S. Sorgenfrei, K. Watanabe, T. Taniguchi, P. Kim, K. L. Shepard, J. Hone, *Nat. Nanotechnol.* **2010**, *5*, 722–726.
[10] a) K. I. Bolotin, K. J. Sikes, J. Hone, H. L. Stormer, P. Kim, *Phys. Rev. Lett.* **2008**, *101*, 096802; b) J. Moser, A. Barreiro, A. Bachtold, *Appl. Phys. Lett.* **2007**, *91*, 163513.
[11] S. Adam, S. Y. Jung, N. N. Klimov, N. B. Zhitenev, J. A. Stroscio, M. D. Stiles, *Phys. Rev. B* **2011**, *84*, 235421.

© 2014 Wiley-VCH Verlag GmbH & Co. KGaA, Weinheim

[12] C. E. Banks, A. Crossley, C. Salter, S. J. Wilkins, R. G. Compton, *Angew. Chem. Int. Ed.* **2006**, *45*, 2533 – 2537; *Angew. Chem.* **2006**, *118*, 2595 – 2599.
[13] a) L. Wang, A. Ambrosi, M. Pumera, *Angew. Chem. Int. Ed.* **2013**, *52*, 13818 – 13821; *Angew. Chem.* **2013**, *125*, 14063 – 14066; b) C. H. A. Wong, C. K. Chua, B. Khezri, R. D. Webster, M. Pumera, *Angew. Chem. Int. Ed.* **2013**, *52*, 8685 – 8688; *Angew. Chem.* **2013**, *125*, 8847 – 8850; c) A. Ambrosi, S. Y. Chee, B. Khezri, R. D. Webster, Z. Sofer, M. Pumera, *Angew. Chem. Int. Ed.* **2012**, *51*, 500 – 503; *Angew. Chem.* **2012**, *124*, 515 – 518; d) S. M. Tan, A. Ambrosi, B. Khezri, R. D. Webster, M. Pumera, *Phys. Chem. Chem. Phys.* **2014**, *16*, 7058 – 7065.
[14] K. Zaghib, X. Song, A. Guerfi, R. Rioux, K. Kinoshita, *J. Power Sources* **2003**, *119*, 8 – 15.
[15] a) R. Munoz, C. Gomez-Aleixandre, *Chem. Vap. Deposition* **2013**, *19*, 297 – 322; b) Y. Zhang, L. Y. Zhang, C. W. Zhou, *Acc. Chem. Res.* **2013**, *46*, 2329 – 2339.
[16] J. Song, F. Y. Kam, R. Q. Png, W. L. Seah, J. M. Zhuo, G. K. Lim, P. K. H. Ho, L. L. Chua, *Nat. Nanotechnol.* **2013**, *8*, 356 – 362.
[17] A. Ambrosi, M. Pumera, *Nanoscale* **2014**, *6*, 472 – 476.
[18] H. K. Yu, K. Balasubramanian, K. Kim, J.-L. Lee, M. Maiti, C. Ropers, J. Krieg, K. Kern, A. M. Wodtke, *ACS Nano* **2014**, *8*, 8636 – 8643.
[19] B. Beverskog, I. Puigdomenech, *J. Electrochem. Soc.* **1997**, *144*, 3476 – 3483.
[20] D. Grujicic, B. Pesic, *Electrochim. Acta* **2002**, *47*, 2901 – 2912.
[21] a) F. K. Crundwell, *Electrochim. Acta* **1992**, *37*, 2707 – 2714; b) S. Zor, M. Saracoglu, F. Kandemirli, T. Arslan, *Corrosion* **2011**, *67*, 125003.
[22] a) D. Tromans, R. H. Sun, *J. Electrochem. Soc.* **1991**, *138*, 3235 – 3244; b) V. Brusic, M. A. Frisch, B. N. Eldridge, F. P. Novak, F. B. Kaufman, B. M. Rush, G. S. Frankel, *J. Electrochem. Soc.* **1991**, *138*, 2253 – 2259.
[23] M. Gross, J. Jordan, *Pure Appl. Chem.* **1984**, *56*, 1095 – 1129.
[24] a) A. L. Bacarell, J. C. Griess, *J. Electrochem. Soc.* **1973**, *120*, 459 – 465; b) B. E. Conway, B. V. Tilak, *Electrochim. Acta* **2002**, *47*, 3571 – 3594.
[25] a) F. Tuinstra, J. L. Koenig, *J. Chem. Phys.* **1970**, *53*, 1126; b) A. C. Ferrari, J. C. Meyer, V. Scardaci, C. Casiraghi, M. Lazzeri, F. Mauri, S. Piscanec, D. Jiang, K. S. Novoselov, S. Roth, A. K. Geim, *Phys. Rev. Lett.* **2006**, *97*, 187401; c) L. G. Cancado, A. Jorio, E. H. M. Ferreira, F. Stavale, C. A. Achete, R. B. Capaz, M. V. O. Moutinho, A. Lombardo, T. S. Kulmala, A. C. Ferrari, *Nano Lett.* **2011**, *11*, 3190 – 3196; d) M. M. Lucchese, F. Stavale, E. H. M. Ferreira, C. Vilani, M. V. O. Moutinho, R. B. Capaz, C. A. Achete, A. Jorio, *Carbon* **2010**, *48*, 1592 – 1597.
[26] M. Bruna, A. K. Ott, M. Ijäs, D. Yoon, U. Sassi, A. C. Ferrari, *ACS Nano* **2014**, *8*, 7432 – 7441.
[27] K. Takeuchi, A. Suda, S. Ushioda, *Surf. Sci.* **2001**, *489*, 100 – 106.
[28] E. J. E. Stuart, M. Pumera, *J. Phys. Chem. C* **2010**, *114*, 21296 – 21298.
[29] a) T. J. Davies, M. E. Hyde, R. G. Compton, *Angew. Chem. Int. Ed.* **2005**, *44*, 5121 – 5126; *Angew. Chem.* **2005**, *117*, 5251 – 5256; b) R. L. McCreery, *Chem. Rev.* **2008**, *108*, 2646 – 2687.

Received: September 23, 2014
Published online on October 21, 2014

© 2014 Wiley-VCH Verlag GmbH & Co. KGaA, Weinheim